International Journal of Nanomedicine

Dovepress

open access to scientific and medical research

Open Access Full Text Article

ORIGINAL RESEARCH

Surface Functionalization with Proanthocyanidins Provides an Anti-Oxidant Defense Mechanism That Improves the Long-Term Stability and Osteogenesis of Titanium Implants

This article was published in the following Dove Press journal:
International Journal of Nanomedicine

Jiahao Tang[1,2]
Liang Chen[1,2]
Deyi Yan[1,2]
Zijian Shen[1,2]
Bingzhang Wang[1,2]
Sheji Weng[1,2]
Zongyi Wu[1,2]
Zhongjie Xie[1,2]
Jiancan Shao[1,2]
Lei Yang[1,2]
Liyan Shen[1,2]

[1]The Second School of Medicine Wenzhou Medical University, Wenzhou, Zhejiang 325000, People's Republic of China; [2]Key Laboratory of Orthopedics of Zhejiang Province, Department of Orthopedics, The Second Affiliated Hospital and Yuying Children's Hospital of Wenzhou Medical University, Wenzhou, Zhejiang 325000, People's Republic of China

Correspondence: Lei Yang; Liyan Shen
Key Laboratory of Orthopedics of Zhejiang Province, Department of Orthopedics, The Second Affiliated Hospital and Yuying Children's Hospital of Wenzhou Medical University, No. 109, Xueyuan West Road, Lucheng District, Wenzhou, Zhejiang 325000, People's Republic of China
Fax +86 577 88002760
Email yl190015@hotmail.com; uynixmm@163.com

Purpose: Aseptic loosening is a major complication after total joint replacement. Reactive oxygen species generated by local tissue cells and liberated from implant surfaces have been suggested to cause implant failures. Surface modification of titanium (Ti)-based implants with proanthocyanidins (PAC) is a promising approach for the development of anti-oxidant defense mechanism to supplement the mechanical functions of Ti implants. In this study, a controlled PAC release system was fabricated on the surface of Ti substrates using the layer-by-layer (LBL) assembly.

Materials and Methods: Polyethyleneimine (PEI) base layer was fabricated to enable layer-by-layer (LBL) deposition of hyaluronic acid/chitosan (HA/CS) multi-layers without or with the PAC. Surface topography and wettability of the fabricated HA/CS-PAC substrates were characterized by scanning electron microscopy (SEM), atomic force microscopy (AFM), Fourier-transform infrared spectroscopy (FTIR) and contact angle measurement. PAC release profiles were investigated using drug release assays. MC3T3-E1 pre-osteoblast cells were used to assess the osteo-inductive effects of HA/CS-PAC substrates under conditions H_2O_2-induced oxidative stress in vitro. A rat model of femoral intramedullary implantation evaluated the osseo-integration and osteo-inductive potential of the HA/CS-PAC coated Ti implants in vivo.

Results: SEM, AFM, FTIR and contact angle measurements verified the successful fabrication of Ti surfaces with multi-layered HA/CS-PAC coating. Drug release assays revealed controlled and sustained release of PAC over 14 days. In vitro, cell-based assays showed high tolerability and enhanced the osteogenic potential of MC3T3-E1 cells on HA/CS-PAC substrates when under conditions of H_2O_2-induced oxidative stress. In vivo evaluation of femoral bone 14 days after femoral intramedullary implantation confirmed the enhanced osteo-inductive potential of the HA/CS-PAC coated Ti implants.

Conclusion: Multi-layering of HA/CS-PAC coating onto Ti-based surfaces by the LBL deposition significantly enhances implant osseo-integration and promotes osteogenesis under conditions of oxidative stress. This study provides new insights for future applications in the field of joint arthroplasty.

Keywords: proanthocyanidins, anti-oxidant, ROS, layer-by-layer methodology, surface modification of titanium, osteogenesis

Introduction

Joint arthroplasty is one of the most commonly performed orthopaedic procedures for the treatment of end-stage degenerative joint diseases. However, aseptic loosening of prosthesis is a major complication after total joint replacement often

requiring revision surgeries. Due to advanced age of patients and the loss of surrounding bone tissue, and the dangers of the revision surgery, prognostic outcomes are often poorer than for primary arthroplasties.[1] Thus, it is now recognized that the prosthetic implant surface with respect to tissue reaction and osseo-integration is a crucial factor for the long-term success of joint arthroplasty. Pure titanium (Ti) and Ti-based materials or alloys have become the most widely used metal implants due to their superiority in load-bearing applications with excellent mechanical strength and resilience.[2–4] Despite these properties, it has been shown that the bioactivity of Ti surfaces is insufficient to induce direct growth of bone tissue and encourage good osseo-integration. Proper implant osseo-integration is necessary for reliable mechanical fixation of the implant. Thus, much attention has been focused on the development of various coatings to supplement the mechanical functions of Ti implants.

Recently it has been reported that the electrochemical redox processes that occur at metallic implant surfaces have a profound effect on the local surrounding tissues and the downstream inflammatory response, with oxidative stress reactions a leading cause of implant failures.[5–8] Although reactive oxygen species (ROS) are normal metabolic by-products, they play important roles in the inflammatory response serving as both signaling and effector molecules.[9–11] Reactive oxygen intermediates produced at implant-bone interfaces serve as strong chemo-attractants for the recruitment of immune cells leading to surrounding tissue damage and fibrosis, whilst ROS produced by immune cells can directly lead to the corrosion of the implants.[12,13] An imbalance between excessive ROS generation and an insufficient anti-oxidant defense mechanism hinders bone-implant osseo-integration further aggravating aseptic loosening. Thus, there is a need for the fabrication of bioactive surface coating with anti-oxidant properties to improve implant osseo-integration, stability, and effective lifespan.

Proanthocyanidins (PAC) are a group of naturally occurring polyphenols bioflavonoids found in vegetables, flowers, fruits and nuts.[14] PAC have been reported to possess broad biological activity including but not limited to anti–viral, anti-microbial, anti-HIV, anti-tumour, cardio-protective, anti-arteriosclerotic and anti-thrombic effects with broad therapeutic applications.[15] Specifically, these biological effects exerted by PAC can be attributed to its potent anti-oxidant properties and have also been recognized to be implicated in the anti-apoptosis effect of PAC.[16,17] Moreover, recent data have shown that PAC can stimulate bone formation and regulate osteoclast bone resorption, thus ideal for the treatment of osteolytic conditions including osteoporosis.[18–22] With such beneficial biological effects, PAC is an ideal candidate for the functionalization of Ti implants to protect against ROS and to enhance osseo-integration.

The objective of this study was to utilize the layer-by-layer (LBL) self-assembly methodology for the surface functionalization of Ti substrate to enable the controlled release of PAC. LBL assembly is a versatile self-assembly technique used for the formulation of polyelectrolyte multilayers (PEMs) via the electrostatic attractions (polyanions and polycations) between the assembled components and has been widely used for surface modification of dental Ti implants.[23] To apply the LBL methodology, the surface of the Ti substrates needs to be charged by the conjugation of polyethylenimine (PEI) base layer to obtain high binding forces. PEI is an efficient polymer carrier with high pH buffering capacity and as such often described as a "proton sponge".[24,25] Multi-layers composed of positively charged chitosan (CS) and negatively charged hyaluronic acid (HA) were deposited onto the PEI layer via the LBL self-assembly. HA/CS is commonly used due to their desirable biocompatibility, biodegradability and potential for controlled drug delivery and release.[26–28] The 3D HA/CS multi-layered network prepared by the LBL method enables the encapsulation of PAC in the micro-interspaces between HA and CS allowing for its sustained and controlled release.

Surface topography analysis by SEM, AFM and water contact angle measurement, chemical analysis of surface coatings by FTIR, and drug release assays was applied for the in vitro characterization of the multi-layered HA/CS coating for incorporation and release of PAC on Ti substrates. The murine pre-osteoblast cell line, MC3T3-E1, with high levels of osteoblast differentiation potential, was used to evaluate the anti-oxidant and osteo-inductive effects of multi-layered HA/CS-PAC coated Ti substrates under conditions H_2O_2-induced oxidative stress in vitro. In addition, the performance of the HA/CS-PAC coated Ti substrates and uncoated pure Ti was evaluated in vivo using a surgical femoral intramedullary implantation model in Sprague Dawley rats. Micro-CT and histology analyses were carried out to assess bone-implant osseo-integration and osteo-induction. This study provides a new insight into the potential application of PAC as an anti-oxidant defense mechanism on the surface of Ti-based

implants for enhanced osseo-integration and new bone formation.

Materials and Methods

Materials

Commercial pure Titanium (Ti; 99% pure) was provided by Baoji Titanium Industry Co. Ltd. (Baoji, Shaanxi, China). Polyethylenimine (PEI; 99%), chitosan (CS; deacetylation degree of 80%, and viscosity of 200 mPas) and proanthocyanidins (PAC) were purchased from Solarbio Life Sciences (Beijing, China). Hyaluronic acid (HA) was obtained from Bloomage Biotechnology Co. Ltd. (Jinan, Shandong, China). Minimum Essential Medium Eagle with Alpha modification (α-MEM), phosphate-buffed saline (PBS), fetal bovine serum (FBS), penicillin-streptomycin, and trypsin were acquired from Thermo Fisher Scientific (Waltham, MA, USA). Specific primary antibodies against p53, Bax, Bcl-2, and β-actin were sourced from Abcam (Cambridge, UK).

Specimen Preparation

Fabrication of the Titanium-PEI Substrate

Ti disks (each with thickness of 0.3 mm and diameter of 14 mm) and Ti rods (each with length of 15 mm and diameter of 1.5 mm) were polished to a reflective mirror-like finish. After polishing, all samples were ultrasonically cleaned with successive washes in acetone, 70% ethanol, and then finally in sterile deionized water. Washed samples were dried for 1 hr at 60°C and then immersed in PEI solution (5 mg/mL in sterile deionized water; pH 9.0) for 20 mins. Following incubation, Ti-PEI substrates were air-dried at room temperature in a ventilated environment for 4 hrs.

Preparation of Layer-by-Layer (LBL) HA/CS-PAC Coatings on the Ti-PEI Substrates

Hyaluronic acid (HA) solution (1 mg/mL; pH 2.9) was prepared in sterile deionized water. The Ti-PEI substrates prepared, as described above, were immersed in the HA solution for 30 mins and then air-dried at room temperature for 4 hrs (denoted Ti-PEI-HA substrates). Chitosan (CS) solution was prepared by dissolving 1 g (w/v; or 0.1%) CS in diluted 1% (v/v) glacial acetic acid with the aid of a magnetic stirrer. Next, PAC at concentrations of 0.5×10^{-3} mol/L (PAC-low), 1×10^{-3} mol/L (PAC-middle), and 2×10^{-3} mol/L (PAC-high) were then prepared by dissolving in the CS solution with constant magnetic stirring. The Ti-PEI-HA substrates were then immersed in CS solution without or with the indicated concentrations of PAC for 30 mins and air-dried at room temperature for 4 hrs. Immersion in HA and CS solution was repeated for a total of 3 cycles to form a multi-layered HA/CS-PAC coating (Figure 1) and then stored under sterile conditions at 4°C until further use. The final substrates Ti-PEI-HA/CS, Ti-PEI-HA/CS-PAC-L, Ti-PEI-HA/CS-PAC-M, and Ti-PEI-HA/CS-PAC-H was denoted as HA/CS, HA/CS-L, HA/CS-M, and HA/CS-H, respectively.

Surface Characterization of Ti Substrates

The typical surface topography and characteristics of Ti, Ti-PEI, Ti-PEI-HA, HA/CS, HA/CS-L were analyzed by scanning electron microscopy (Hitachi S-4800 SEM, Hitachi Ltd., Tokyo, Japan). The chemical composition of all Ti substrates was measured using fourier transform infrared (FTIR) spectroscopy (Thermo Nicolet NEXUS 470 FTIR, Thermo Fisher Scientific) in transmission mode scanning within the range of 400–4000 cm^{-1}. The JPK nanoWizard II atomic force microscopy system (JPK BioAFM, Berlin, Germany) was used to characterize the surface roughness of Ti, HA/CS and HA/CS-L substrates. Wettability was measured by the deionized water contact angle (wetting angle) measurement using a Digidrop Contact Angle Meter (GBX, France). A drop volume of 2 μL was used and drop images were acquired on a OCA 25 system equipped with digital camera, and contact angle measurements analyzed using the systems analysis software (SCA 20 module, Data Physics Instruments GmbH, Filderstadt, Germany).

In vitro Drug Release Profiles

Standard curves based on known concentrations (0, 0.01, 0.02, 0.039, 0.078, 0.156, 0.3125, 0.625, 1.25, 2.5, and 5 mg/mL) of PAC in PBS were generated using OD readings obtained by ultraviolet-visible double beam spectrophotometer (Mapada UV6100s, Shanghai Mapada Instruments Co., Ltd, Shanghai, China). The subsequent PAC concentration released from the HA/CS substrates was calculated based on the standard curve. Drug release profiling experiments were performed at 37°C by immersing the HA/CS-L, HA/CS-M, or HA/CS-H substrates in PBS (pH 7.4). At the predetermined time-points (per day), substrates were removed and the PBS solutions were analyzed by ultraviolet-visible spectrophotometry. The substrates were immersed in fresh PBS and incubated until the next time-point. Testing period lasted for 14 days. The percentage of PAC release was calculated by dividing the accumulated amount of released PAC by the total amount of PAC released at the end of the experimental period.

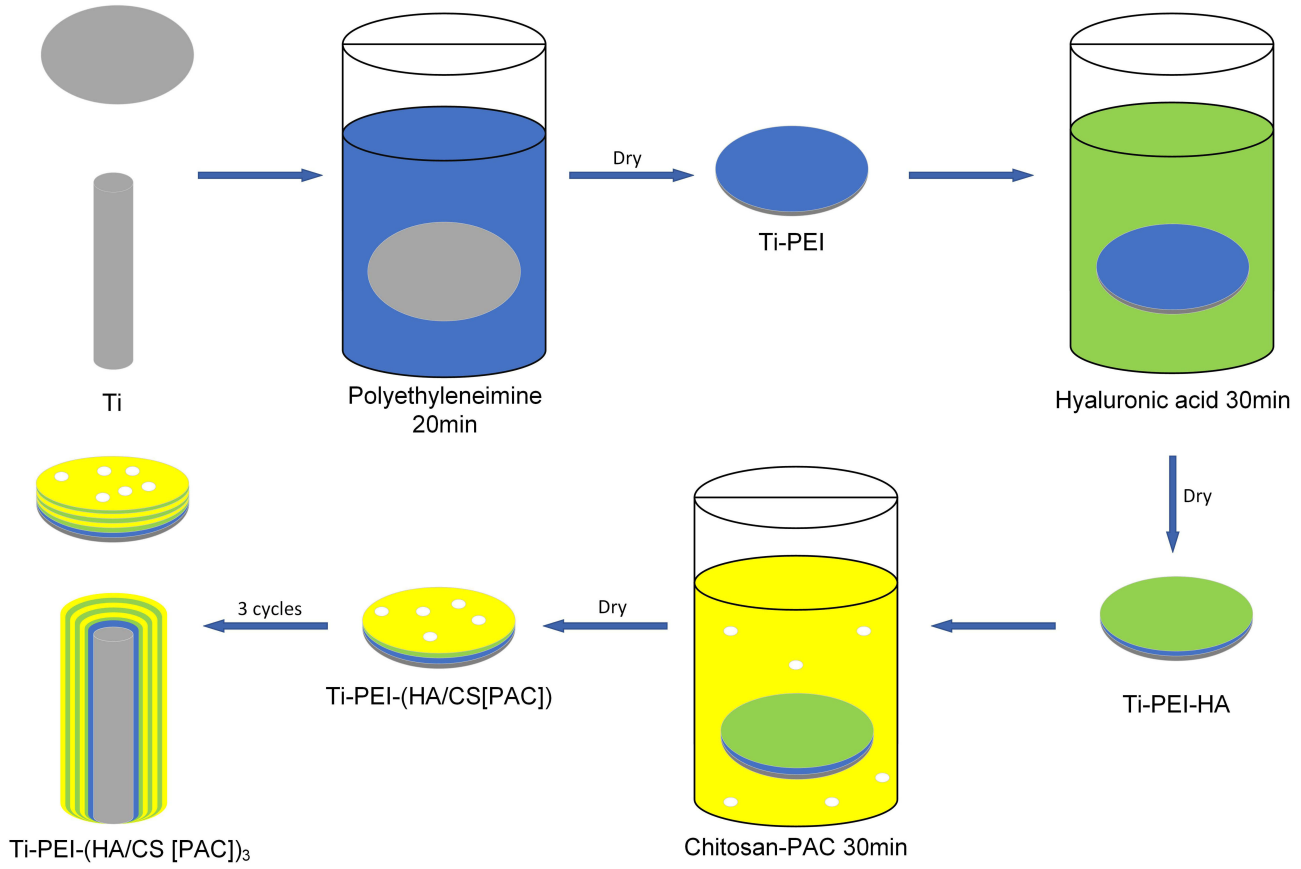

Figure 1 Schematic diagram of sample preparation: the process of fabricating the HA/CS-PAC multilayer coatings on the PEI-primed Ti disk or rod surfaces.
Abbreviations: CS, chitosan; HA, hyaluronic acid; PAC, proanthocyanidins; PEI, polyethyleneimine; Ti, titanium.

In vitro Cellular and Biochemical Analyses

Cell Culture

H_2O_2 (30%, w/w) was purchased from Sigma-Aldrich (St. Louis, MO, USA), and diluted with α-MEM to a final concentration of 300 μM before use. Mouse pre-osteoblastic cell line MC3T3-E1 cells were obtained from the ATCC (Manassas, VA, USA) maintained in α-MEM supplemented with 10% FBS and 1% penicillin-streptomycin (complete α-MEM) at 37°C under humidified condition of 5% CO_2. Oxidative stress was induced by treating MC3T3-E1 cells with 300 μM H_2O_2. The Ti substrates (Ti, HA/CS, HA/CS-L, HA/CS-M, and HA/CS-H) were sterilized using a 25 kGy dose of gamma radiation from cobalt-60 (Wenzhou Gaoke Fuzhao Co., Zhejiang, China) prior to seeding of cells onto the substrate surface. MC3T3-E1 cells were seeded onto Ti substrates at a density of 1×10^4 cells/well.

Antioxidant Activity of Ti Substrates Using FRAP Assay

The total antioxidant capacity of different Ti substrates was measured using the ferric reducing antioxidant power (FRAP) assay kit (Beyotime Institute of Biotechnology, China).[29] Typically, a sample was exposed to 200 μL of FRAP working solution at 37°C for 5 mins. The absorbance at 593 nm was then measured on a microplate spectrophotometer (Multiskan FC Microplate Photometer, Thermo Fisher Scientific). An aqueous solution of $FeSO_4$ in the range of 0.15–15mM was used for calibration. The antioxidant activity of each Ti sample was then calculated based on the standard curve. Native Ti substrate was used as controls.

Intracellular ROS Measurement

To oxygen radicals scavenging capacity of cells grown on the Ti substrates were assessed using ROS assay kits based on either 2′,7′-dichlorodihydrofluorescein diacetate (DCFH-DA) or dihydroethidium (DHE). Briefly, MC3T3-E1 cells (1×10^4 cells/cm^2) with H_2O_2 treatment were seeded onto the various Ti substrates for 24 hrs. Cells were then incubated with DCFH-DA (10 μM) or DHE (5 μM) for 20 mins in the dark. DCFH-DA or DHE fluorescence was captured from 4 random fields on a Leica DMI 6000B inverted fluorescent microscope (Leica Microsystems, Wetzlar, Germany). The average fluorescence intensity from each

sample was quantitatively determined using ImagePro Plus 6.0 software (Media Cybernetics, Silver Spring, MD, USA). Three independent repeats were conducted.

Osteogenic Differentiation of MC3TE-E1 Cells on Ti Substrates in vitro

Osteogenic differentiation of MC3T3-E1 cells seeded onto Ti substrates was carried out by culturing cells in complete α-MEM containing 0.1μM dexamethasone, 50μM ascorbate acid, and 10mM β-glycerophosphate, for 14 days. Media were replaced with fresh osteogenic induction media every 2 days. After 14 days culture, ALP activity was evaluated using an ALP staining kit (Beyotime Institute of Biotechnology, Shanghai, China) according to the manufacturer's protocol. Stained cells were imaged under a light microscope.

Cell Proliferation Assay

Cell proliferation was assessed using the CCK-8 Cell Proliferation Cytotoxicity Assay kit according to the manufacturer's instructions (Dojindo Molecular Technologies Inc, Kumamoto, Japan) 14 days after seeding of cells onto Ti substrates. The absorbance of the CCK8 substrate at 450 nm for each experimental condition was measured using a microplate spectrophotometer (Multiskan FC Microplate Photometer, Thermo Fisher Scientific).

Western Blot Analyses

Total cellular proteins were extracted from MC3T3-E1 cells cultured under osteogenic conditions for 14 days using RIPA lysis buffer supplemented with protease and phosphatase inhibitors. Protein concentrations were quantified using bicinchoninic acid (BCA) assay according to the manufacturer's protocol (Pierce, Rockford, IL, USA). Protein samples were subsequently denatured by boiling at 95°C for 5 mins and then 30 μg of proteins was resolved on 10% SDS-PAGE gel. Separated proteins were electroblotted onto PVDF membranes overnight at 4°C. After blocking with 5% skim-milk in TBST (0.1% Tween 20 in Tris-buffered saline) for 1 hr, membranes were incubated with primary antibodies (diluted 1:1000 in 1% skim-milk in TBST) overnight at 4°C. After extensive washed with TBST, membranes were incubated with appropriate horseradish peroxidase-conjugated secondary antibodies (diluted 1:1000 in 1% skim-milk in TBST) for 1 hr at room temperature. The immuno-reactivity of protein-antibody complexes was detected and imaged following exposure to ECL substrate on a gel image-processing system.

In vivo Animal Experiments

Ethics Statement and Experimental Animals

All animal procedures conducted in this study were approved and followed the guidelines of the Institutional Animal Care and Committee Guide of the Animal Research Committee of Wenzhou Medical University. Forty 3-month-old female Sprague Dawley (SD) rats were maintained in isolator cages (4 rats/cage) under specific pathogen-free environment with 12 hrs light/dark cycle at regulated temperatures of 22–24°C and 50–55% humidity. Standard laboratory rodent chow and water were provided adlibitum. All animals were acclimatized for 7 days before their participation in experiments.

Femoral Intramedullary Implantation of Ti Substrates

Surgical femoral intramedullary implantation of Ti substrates was carried out on SD rats as previously described,[30] Briefly, rats were anesthetized by intraperitoneal injection with pentobarbital sodium (50 mg/kg body weight), and prepared for surgery by shaving both hind legs and disinfecting them with 75% alcohol. A medial incision was made to both hind legs of the rats, on the lateral side of the knee to expose the knee joints. A channel of 2 mm in diameter was drilled from the patellofemoral groove of the distal femur along the axis of the femoral shaft into the medullary canal. Sterilized Ti rods coated with HA/CS without or with different concentrations of PAC was inserted via the channel into the medullary canal. During implantation of Ti substrates, the knee joint was lavaged with physiological saline to keep the surface of the joint wet and to rinse out bony debris and dust from the drilling. The joint was closed with biodegradable sutures and all rats were housed in an environmentally controlled animal care laboratory after surgery. No postoperative antibiotic treatment was given and natural movement of the operated legs was observed after surgery. Rats divided into 4 groups according to the coating on the Ti rods: uncoated Ti rods (control), Ti rods coated with HA/CS, Ti rods coated with HA/CS-PAC (HA/CS-L, HA/CS-M, and HA/CS-H).

Micro-CT Evaluation

Two weeks after implantation of Ti substrates, all rats were sacrificed and femoral bones resected, cleaned of soft tissues and then fixed in 4% form aldehyde for 48 hrs at 4°C. The fixed femoral bone samples were analyzed on a Scanco μCT 100 high-resolution μCT

scanner (Scanco Medical, Brüttisellen, Switzerland). Image acquisition was carried out at a voltage of 70 kV, an electric current of 114 μA, and isotropic voxel resolution of 10 μm. Multi-level thresholding was applied to discriminate bone from other tissues or structures, with the threshold for bone at 205 and threshold for implant at 700. Three-dimensional (3-D) reconstructions and quantitative evaluation were conducted using associated software. The volume of interest (VOI) including the trabecular bone around the implant was defined as 2 mm below the highest point of the growth plate to 100 slices distal to the growth plate. Morphometric parameters of bone volume/tissue volume ratio (BV/TV), trabecular number (Tb.N, mm^{-1}), trabecular thickness (Tb.Th, μm), trabecular separation (Tb.Sp, mm), connectivity density (Conn.D, mm^{-3}) and bone mineral density (BMD, $mg/HA/cm^3$) were calculated.

Histological Analysis

Following μCT scanning, all fixed femoral bone tissues were decalcified in 10% EDTA for 2 months at 4°C. Next, the Ti implants were removed from the femurs by gently pushing the implants out along the axis of the femoral bone. Bone tissues were then dehydrated in graded ethanol and embedded in paraffin for ultra-thin sectioning. Longitudinal sections of 5 μm thick were prepared for H&E and Masson's trichrome staining. Stained sections were imaged under light optical microscope equipped with a digital camera (Eclipse NI-E; Nikon Instruments Inc, Tokyo, Japan). Bone apposition analysis was performed using an image analyzer (Image Pro-Plus 6.0; Media Cybernetics, Silver Spring, MD, USA) to evaluate new bone formation in defined areas based on H&E staining. The results were expressed as the area percentage of bone formation (BF%). The BF% was defined as the area of newly formed bone divided by the defect area extending 100 μm from the implant surface.[29]

Statistical Analyses

All data presented in this study are expressed as the mean ± standard deviation (SD) of at least three independent experiments. Statistical analyses were performed with the SPSS 18.0 statistics package (IBM Corporation, NY, USA) and bar graphs were generated using GraphPad Prism 7.0 software (San Diego, CA, USA). Significant differences among groups were determined using unpaired Student's *t*-test or one-way analysis of variance (ANOVA) with post-analysis by Tukey's honest significance test. A p value less than 0.05 was considered statistically significant.

Results

Surface Characterization of Ti Substrates

The surface topography of the Ti substrates was examined under SEM. As shown in Figure 2A, the surface of the pure Ti substrate exhibits a relatively smooth consistent texture and the assembly of one PEI layer did not change much of the surface structures at the micrometer scale (Figure 2B). Similarly, the Ti-PEI-HA substrate (Figure 2C) and the Ti-PEI-HA with single CS (Figure 2D) exhibited the smooth surface characteristics comparable to that of pure Ti substrate. On the other hand, the multiple layers of HA/CS coating on the Ti-PEI substrate (Figure 2E) presented with the same rough striated surface patterning as Ti-PEI-HA substrate. Finally, the deposited PAC were observed to be monodispersed with coarse projection-like characteristics on the surface of the Ti-PEI-HA/CS substrates (Figure 2F), indicating the successful generation of the multi-layered CS-PAC coating onto the Ti-PEI-HA substrate surface.

To further investigate the surface topography in sub-micrometer scale and analyze the surface roughness, AFM was also applied. The characterization showed that compared to pure Ti substrate which exhibited a root mean square (RMS) of 96.5 nm (Figure 2G), the surface contour of the HA/CS multilayer-coated Ti substrate (HA/CS) was less rough with a RMS of 50.3 nm (Figure 2H). The HA/CS-PAC Ti substrate exhibited an even smoother surface with a RMS of 35.7 nm (Figure 2I). The surface smoothness of the HA/CS-PAC Ti substrate could be attributed to the intercalation of PAC particles between the multilayers. These results show that the HA/CS multilayers and PAC particles were successfully and uniformly deposited onto the Ti substrates.

To further verify the PAC species were successfully incorporated into the HA/CS multilayered films, FTIR spectra analysis was carried out. The FTIR spectrum for pure Ti (A), Ti-PEI substrate (B), HA/CS substrate (C) and HA/CS-PAC substrate (D) are shown in Figure 3 and the main absorbance peaks and their correspondent attributions are summarized in Table 1. Pure Ti substrates do not show any noticeable peaks within the absorption range analyzed (400–4000 cm^{-1}). The weak absorption peak at 3316 cm^{-1} indicates tertiary amine of the PEI layer. The broad peaks at 3225 cm^{-1} and at 1072 cm^{-1} suggested

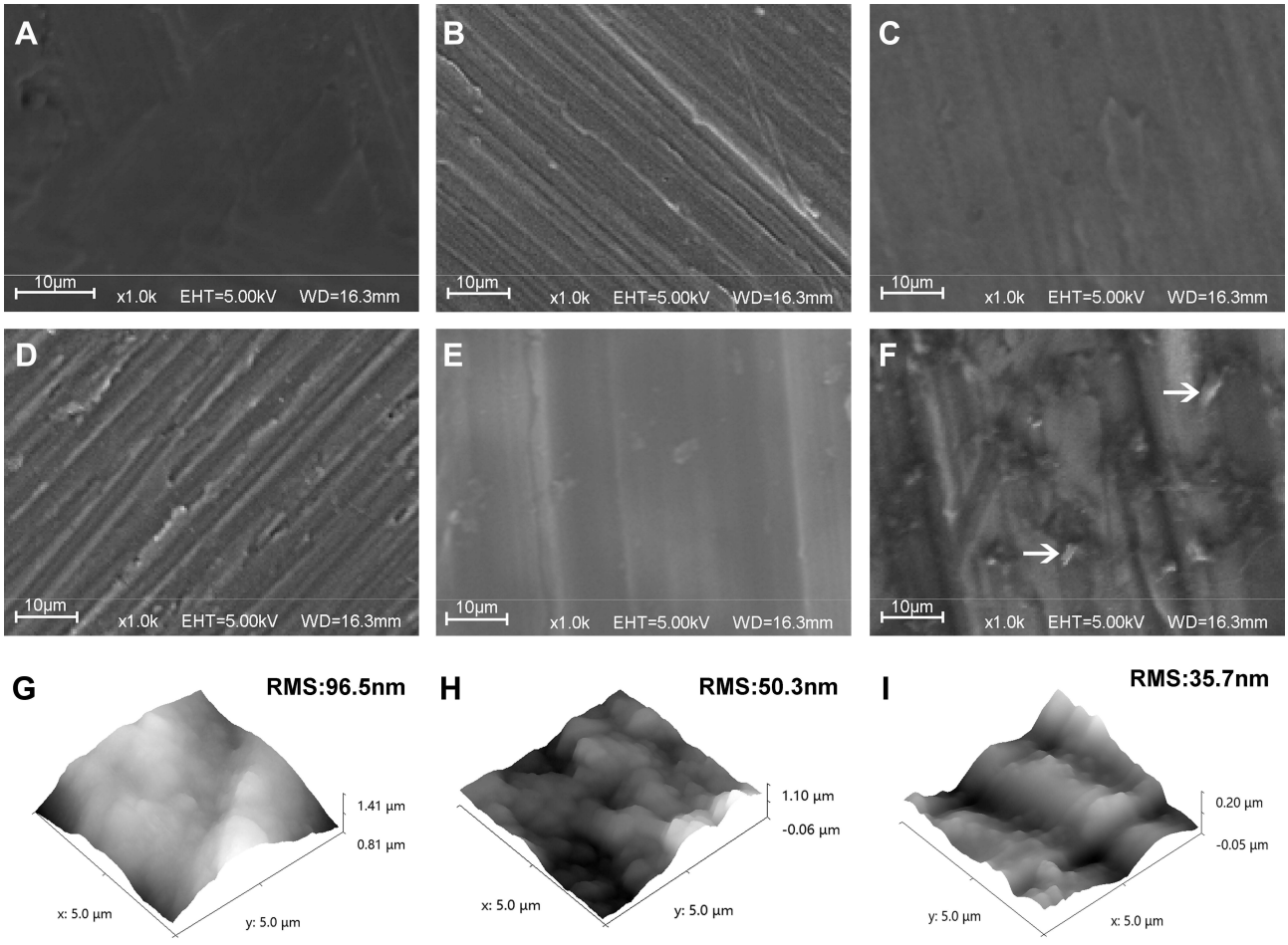

Figure 2 SEM and AFM images of different surfaces.
Notes: SEM or AFM images of (**A&G**) Ti; (**B**) Ti-PEI, Ti after PEI priming; (**C**) Ti-PEI-HA, Ti-PEI after single HA coating; (**D**) Ti-PEI-HA-CS, Ti-PEI after HA-CS coating; (**E&H**) HA/CS, Ti-PEI coated with multilayer of HA-CS; (**F&I**) HA/CS-L, Ti-PEI coated with multilayer of HA-CS with PAC-low immobilization. Arrow indicates agglomerated PAC
Abbreviations: CS, chitosan; HA, hyaluronic acid; PAC, proanthocyanidins; PEI, polyethyleneimine; Ti, titanium.

a surface that was rich in hydroxyl groups and saccharide rings respectively, indicative of the HA/CS coating. The peak at 1611 cm^{-1} signified the amino groups in HA/CS coating. The peak at 1572 cm^{-1} denoted the existence of benzene ring of PAC species. The FTIR spectra results confirmed the successful conjugation of multilayered HA/CS-PAC coating on Ti-PEI substrates.

The hydrophilicity of implants is an important factor that affects the adhesion, biological behaviors, and osteoconductivity of osteoblasts.[31] Water contact angle test was carried out to measure the hydrophilic properties of the prepared substrates, including pure Ti, Ti-PEI, HA/CS and all three HA/CS-PAC (HA/CS-L, HA/CS-M and HA/CS-H) substrates. As shown in Figure 4, coating of Ti surface with either PEI or PEI-HA/CS significantly decreased the water contact angles and increased hydrophilicity as compared to pure Ti substrate. The contact angle of Ti decreased from 76.7° ± 1.9° to 55.4° ± 0.9° following the coating of PEI onto the Ti surface. The contact angle further decreased to 51.4° ± 1.8° when HA/CS was layered onto the Ti-PEI surface. This further decrease in contact angle and increase in hydrophilicity could be attributed to the presence of positive charge amino functional groups of CS and water absorbable HA molecules. Interestingly, the coating of PAC onto the surface of Ti-PEI-HA/CS substrates dose-dependently increased the water contact angles (hence decreased hydrophilicity) of the substrates when compared to either Ti-PEI or Ti-PEI-HA/CS substrates. The contact angle of HA/CS-L, HA/CS-M and HA/CS-H was 58.7° ± 1.4°, 63.1° ± 1.6° and 67.1° ± 1.4°, respectively. Despite showing higher water contact angles than either Ti-PEI or Ti-PEI-HA/CS substrates, incorporation of PAC still resulted in significantly lower water contact angle than pure Ti substrates. Thus, the

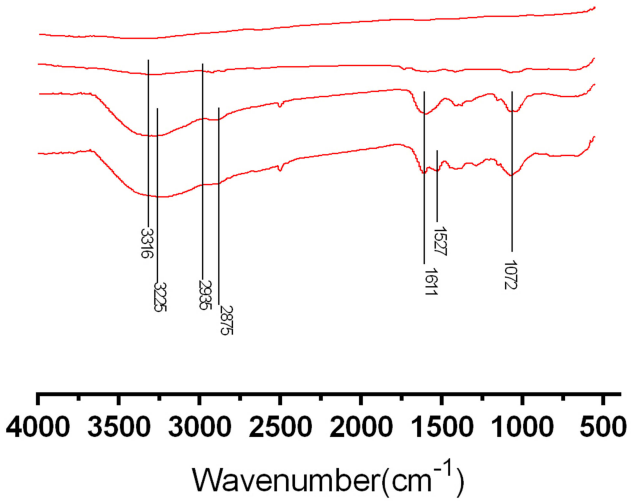

Figure 3 Surface chemical composition analyses by FTIR.
Notes: FTIR wide scan spectra of (**A**) Ti; (**B**) Ti-PEI, Ti after PEI priming; (**C**) HA/CS, Ti-PEI coated with multilayer of HA-CS; (**D**) HA/CS-PAC, Ti-PEI coated with multilayer of HA-CS with PAC-low immobilization
Abbreviations: CS, chitosan; HA, hyaluronic acid; PAC, proanthocyanidins; PEI, polyethyleneimine; Ti, titanium.

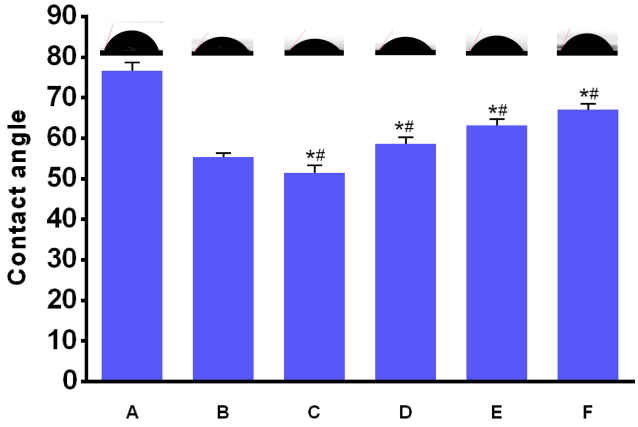

Figure 4 Contact angles of various samples.
Notes: (**A**), Ti; (**B**), Ti-PEI; (**C**), HA/CS; (**D**), HA/CS-L; (**E**), HA/CS-M; (**F**), HA/CS-H. Data are expressed as mean±SD (n=3). *A statistical significance compared to the Ti group ($P<0.05$). #A statistical significance compared to the Ti-PEI group ($P<0.05$).
Abbreviations: CS, chitosan; HA, hyaluronic acid; HA/CS-H, proanthocyanidins-high dose; HA/CS-L, proanthocyanidins–low dose; HA/CS-M, proanthocyanidins-middle dose.

immobilization of multi-layer HA/CS-PAC onto Ti-PEI surface improves the hydrophilicity of pure Ti surface suggesting better cell adhesion effects.

In vitro PAC Release Profile

We next assessed the release behavior of PAC from the HA/CS-PAC substrates over 14 days. As shown in Figure 5A, the cumulative release amount of PAC was dependent on the starting concentration PAC used in the HA/CS-PAC depositing solution. That is, HA/CS-H exhibited the highest cumulative release amount of PAC over the 14-day period and HA/CS-L exhibited the lowest cumulative release amount, with the release for HA/CS-M substrate being in between. The release of PAC from the HA/CS-L substrate was much faster, with 80% of PAC released within the first 5 days (Figure 5B). On the other hand, it took around 10 days for 80% of PAC to be released from either HA/CS-M or HA/CS-H substrates. Together, these results indicate that the HA/CS-L substrates displayed a faster drug release profile, while the HA/CS-M and HA/CS-H substrates showed more sustained drug release behavior.

Table 1 Attribution of the Main Bands of PEI, HA, CS and PAC Analyzed by FTIR in ATR Mode

Chemical Bonds	Wavenumber (cm^{-1})	Corresponding Chemicals
V_{N-H}	3316	PEI and CS
V_{O-H}	3225	HA, CS and PCA
V_{C-H}	2935, 2875	PEI, HA and CS
V_{C-O-C} ring mode	1072	HA and CS
V_{C-O}^{-}(-COO^{-})	1611	HA
Benzene ring	1572	PAC

Abbreviations: CS, chitosan; HA, hyaluronic acid; PAC, proanthocyanidins; PEI, polyethyleneimine; Ti, titanium.

Anti-Oxidative Effects of HA/CS-PAC Substrates

Ferric reducing antioxidant power (FRAP) assay is a widely used method to determine the anti-radical activity of anti-oxidant substrates. This assay is not dependent on the enzymatic/non-enzymatic method to generate free radical prior to evaluation of the anti-radical activity of antioxidants. The assay measures the reduction of ferric iron (Fe^{3+}) to ferrous iron (Fe^{2+}) by anti-oxidants present in experimental samples. Thus, we employed the FRAP assay to analyze the anti-oxidant activity of the various fabricated Ti substrates using pure Ti substrate as controls. Anti-oxidant activity was measured at 7 and 14 days after preparation. As shown in Figure 6A, a dose-dependent increase in total anti-oxidant activity of PAC-loaded HA/CS substrates was observed (HA/CS-L < HA/CS-M < HA/CS-H) when compared with pure Ti substrate and HA/CS substrate without PAC loading. This indicates that the PAC component contribute significantly to the anti-oxidant activity of the HA/CS-PAC substrates. More importantly, significant anti-oxidant activities were retained 14 days after fabrication, which is an important consideration for clinical applications.

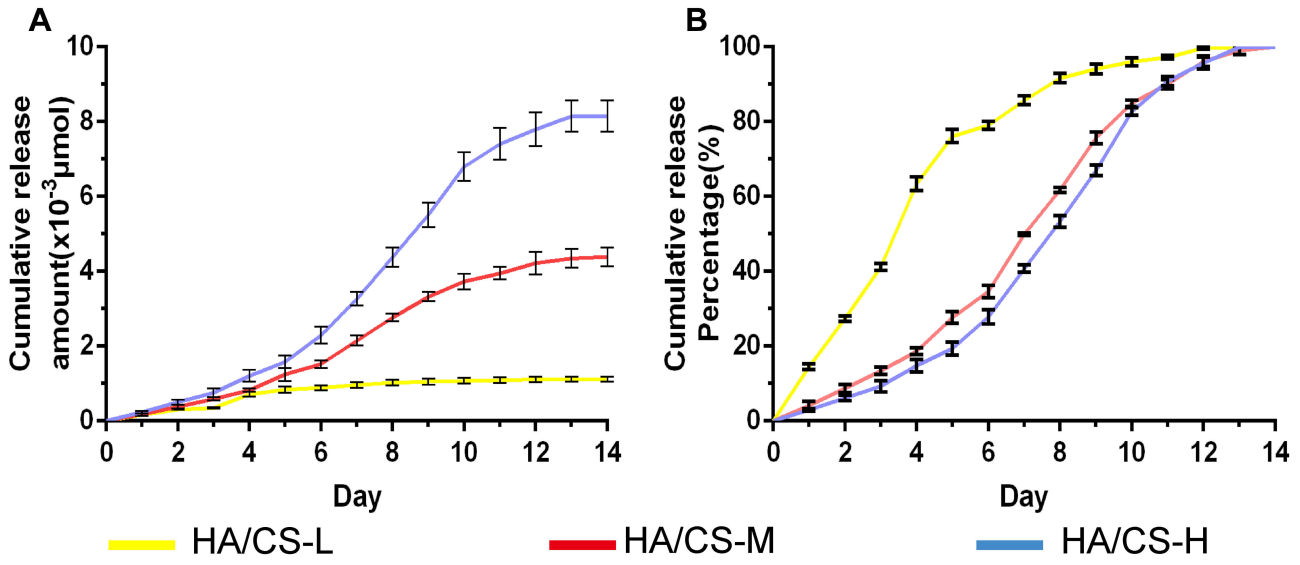

Figure 5 In vitro release profile of HA/CS multilayer surfaces with different concentrations of PAC.
Notes: (**A**) Cumulative release amount. (**B**) Cumulative release percentage. Data are expressed as mean ± SD (n=3).
Abbreviations: CS, chitosan; HA, hyaluronic acid; HA/CS-H, proanthocyanidins-high dose; HA/CS-L, proanthocyanidins-low dose; HA/CS-M, proanthocyanidins-middle dose.

Suppression of Intracellular ROS Levels in MC3T3-E1 Cells Cultured on HA/CS-PAC Substrates

The ability of HA/CS-PAC to suppress intracellular ROS production in cultured MC3T3 cells under H_2O_2-induced oxidative stress conditions was examined using DCFH-DA (Figure 6B and D) and DHE fluorescence-based ROS assays (Figure 6C and E). Under H_2O_2-induced oxidative stress, marked elevations in intracellular ROS were detected in cells cultured on pure Ti and HA/CS substrates (Figure 6B-E). However, a dose-dependent decrease in intracellular ROS production was observed when cells were cultured on the PAC-loaded HA/CS substrates. These results provided further evidence that the HA/CS-PAC multilayered substrate can effectively inhibit the intracellular ROS production in MC3T3 osteoblasts, thus alleviating the detrimental effects of oxidative injury caused by H_2O_2 exposure.

In vitro Osteoblast Differentiation of MC3T3-E1 Cells

We next assessed whether PAC coated HA/CS substrates impacted osteo-induction in the presence of oxidative stress. MC3T3-E1 cells were cultured on HA/CS or HA/CS-PAC substrates under osteogenic condition and in the presence of H_2O_2 for 14 days after which ALP activity was evaluated. Compared to the pure uncoated Ti substrate and HA/CS substrate without PAC, the ALP activity was enhanced in the PAC coated HA/CS substrates in particular the HA/CS-M substrate (Figure 7A and B). Thus collectively, the results indicated that cells cultured on PAC coated HA/CS substrate exhibit stronger differentiation potential than cells cultured on HA/CS substrate alone when in the presence of oxidative stress. This suggests that PAC exerts potent anti-oxidant effects against the deleterious consequence of oxidative stress on osteoblastic precursor cell differentiation.

In vitro MC3T3-E1 Cell Proliferation

The CCK-8 assay is used to assess both cell viability and cell proliferation. The amount of the formazan dye, generated by the dehydrogenase reduction of the water soluble CCK8 reagent WST8 in cells, is directly proportional to the number of living cells and also proportional to cellular proliferation. As PAC possesses potent anti-oxidative effects, cells were cultured onto substrates coated with HA/CS without or with different concentrations of PAC in the presence of H_2O_2 for 14 days after which cell viability/proliferation was assessed. As shown in Figure 7C, cells cultured on HA/CS substrates loaded with medium to high concentrations of PAC exhibited a higher level of cellular proliferation than cells cultured on HA/CS alone or on HA/CS with low PAC concentration. This suggests that cells cultured on substrates with higher PAC concentration were more protected against the detrimental effect of oxidative stress induced by H_2O_2 and appears to be beneficial to the proliferation of the cells.

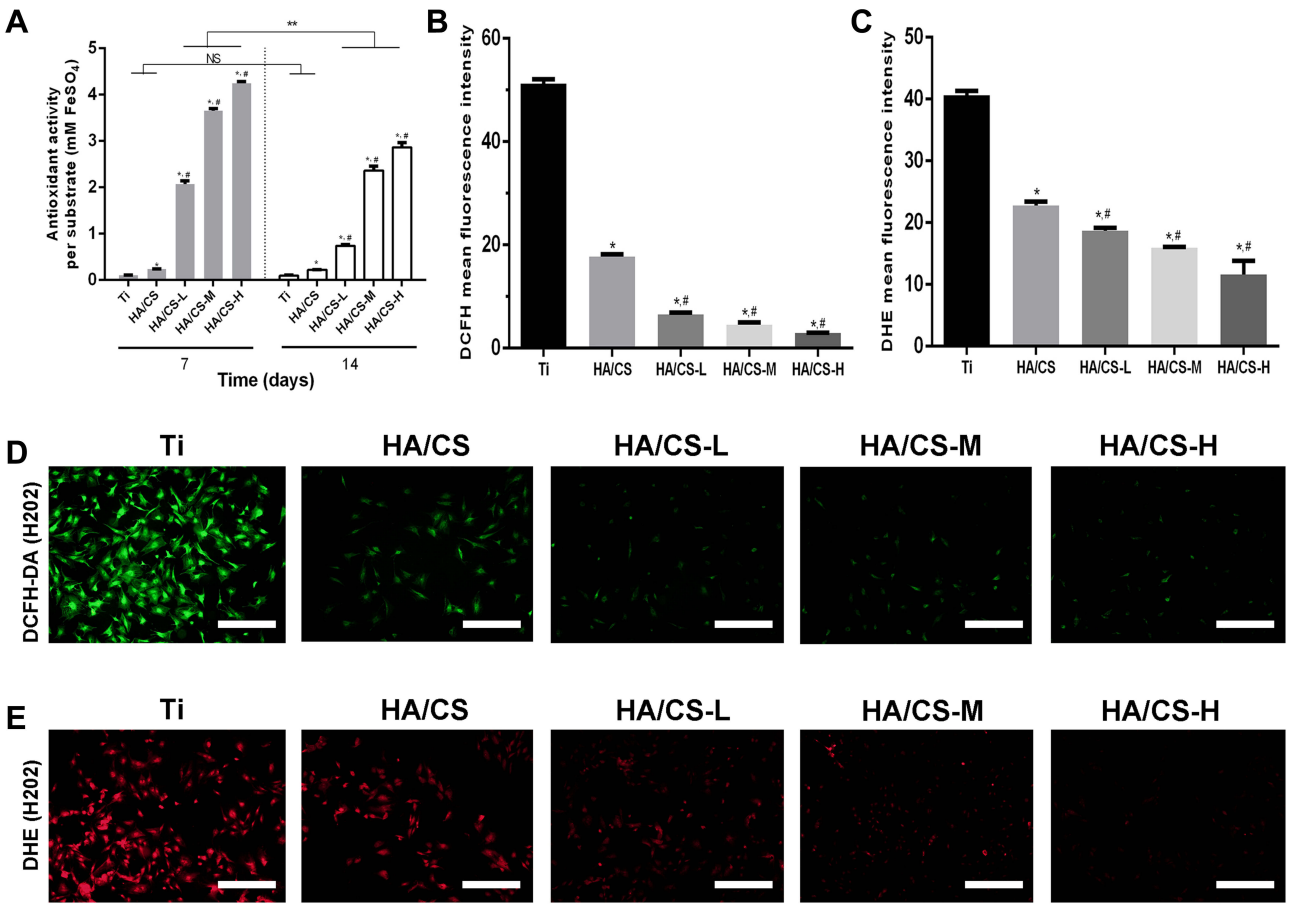

Figure 6 Antioxidant potential characterization.

Notes: (**A**) antioxidant activity of different Ti substrates; (**B&C**) quantitative fluorescence intensity analysis based on images of D&E; (**D&E**) fluorescence images of intracellular ROS of osteoblasts grown onto different Ti substrates staining with DCFH-DA and DHE, respectively (Scale bar =100 μm). Data are expressed as mean ± SD (n=3). *A statistical significance compared to the Ti group ($P<0.05$). #A statistical significance compared to the HA/CS multilayer group ($P<0.05$). **p < 0.01

Abbreviations: CS, chitosan; HA, hyaluronic acid; HA/CS-H, proanthocyanidins-high dose; HA/CS-L, proanthocyanidins-low dose; HA/CS-M, proanthocyanidins-middle dose; NS, no significance.

HA/CS-PAC Substrates Inhibit P53-Induced Apoptosis in MC3T3-E1 Cells

We next investigated the potential molecular mechanism for the protective effects of HA/CS-PAC substrates against H_2O_2-induced oxidative stress and survival of MC3T3-E1 cells. The p53-mediated signal transduction pathway[32] whereby the induction of the pro-apoptotic inducer Bax and down-regulation of anti-apoptotic effect Bcl-2[33] have been shown to be targets of the anti-apoptotic effect of procyanidins. Thus, we examined the expression of these proteins in MC3T3-E1 cells cultured on the various HA/CS substrates and following exposure to H_2O_2. As shown in Figure 8A and B, H_2O_2 treatment significantly induced the expression of p53 and Bax protein in cells cultured on pure Ti and HA/CS substrates. Consistent with elevation in p53 and Bax, the expression of Bcl-2 in cells cultured on these substrates was markedly reduced (Figure 8A and D). On the other hand, cells cultured on HA/CS-PAC substrates revealed inhibition of p53 and Bax induction following H_2O_2 treatment, whereas the anti-apoptotic Bcl-2 protein expression was significantly elevated in a dose-dependent manner (Figure 8A–D). Collectively, these results suggested that the protective effects of the HA/CS-PAC substrates against H_2O_2-induced oxidative stress and cell injury are in part due to inhibition of p53-Bax-mediated apoptosis.

New Bone Formation and Osseo-Integration of HA/CS-PAC Substrates in vivo

The in vivo osteo-inductivity of the HA/CS Ti substrate (in the form of Ti rods) without or with PAC loading was evaluated using the rodent femoral intramedullary implantation model. Two weeks after implantation of the substrates, rats were sacrificed, femurs with substrate implants

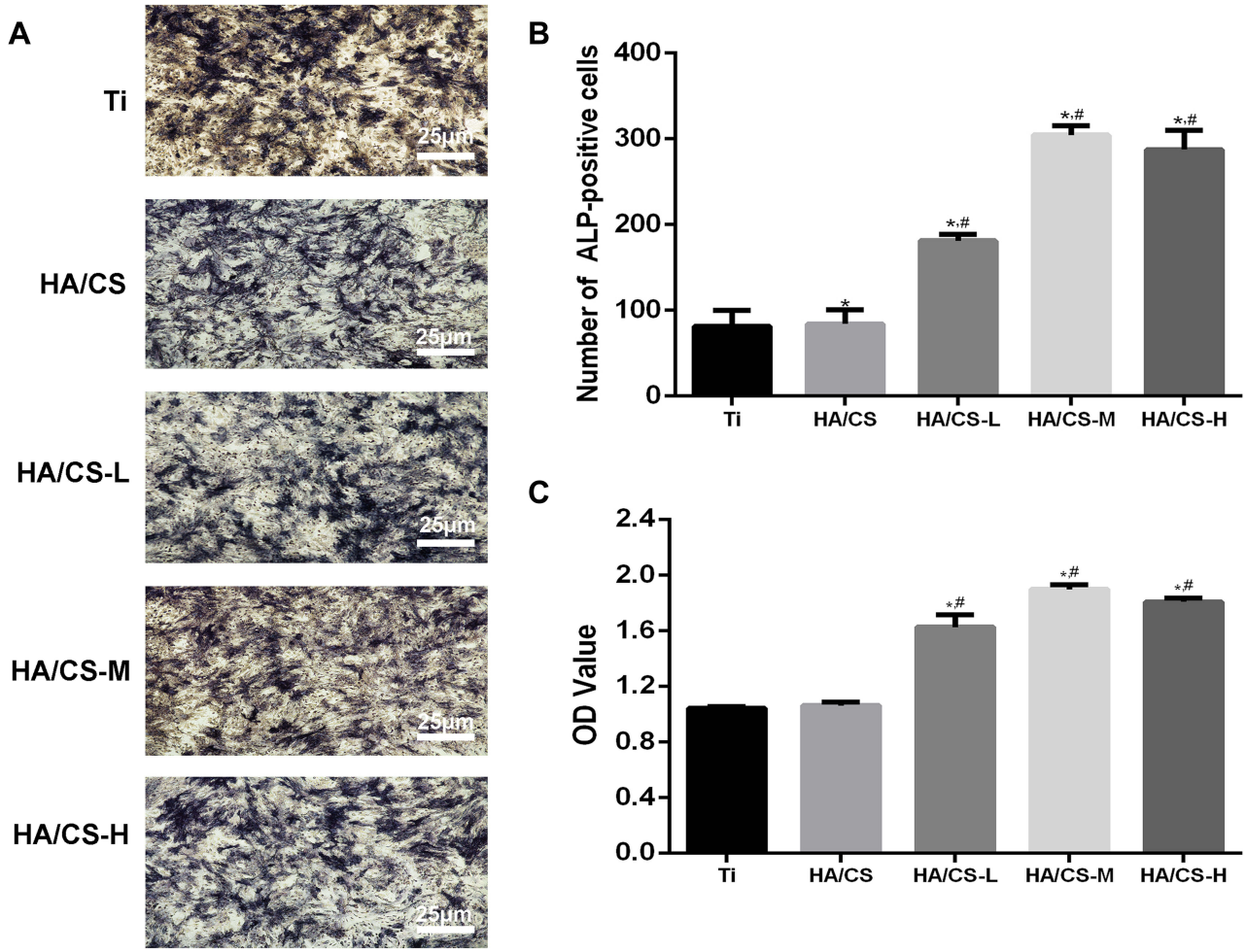

Figure 7 In vitro ALP activity and osteogenic proliferation of MC3T3-E1 cells cultured on different surfaces.
Notes: (**A&B**) The ALP activity (40x); (**C**) The CCK-8 assay. Data are expressed as mean ± SD (n=3). *A statistical significance compared to the Ti group ($P<0.05$). #A statistical significance compared to the HA/CS multilayer group ($P<0.05$).
Abbreviations: CCK-8, cell counting kit-8; ALP, alkaline phosphatase; CS, chitosan; HA, hyaluronic acid; HA/CS-H, proanthocyanidins-high dose; HA/CS-L, proanthocyanidins-low dose; HA/CS-M, proanthocyanidins-middle dose.

were subjected to μCT analysis (Figure 9). Compared to the uncoated pure Ti group and HA/CS without PAC group, the peri–implant bone volume was significantly higher in the PAC coated HA/CS groups, particularly in the HA/CS-H group (Figure 9A). Quantitative morphometric analyses of peri–implant bone mineral density (BMD), bone volume fraction (BV/TV) and associated trabecular bone parameters including trabecular number (Tb.N), trabecular spacing (Tb.Sp), trabecular thickness (Tb.Th), and connectivity density (Conn.D) confirmed the elevated new bone formation of the HA/CS-PAC substrates with HA/CS-H showing the most potent osteoinductive effect (Figure 9B–G).

Histological assessments were then carried out to further examine the level of peri–implant new bone formation. After careful extraction of the Ti rods from femoral bone, the bone tissues were decalcified and processed for H&E and Masson's trichrome staining. As expected varying degrees of new bone formation were observed as shown in Figure 9. In the uncoated Ti substrate control group, non-mineralized fibrous tissues were observed surrounding the uncoated Ti implants, with no apparent new bone formation directly adjacent to the implant surface (Figure 10A, B, E, and F). In contrast, the HA/CS loaded with PAC showed abundant new trabecular bone and osteoid formation directly adjacent to the substrate consistent with the μCT findings. Additionally, numerous osteoblasts were observed to line the apparent newly formed bone (Figure 10C, D, G, and H). The BF% of the PAC group was significantly higher than that of the Ti group after 2 weeks of implantation (Figure 8I). BF% was 36.4%±3.8% in the PAC group, higher than 27.2%±1.3% in the Ti group (P<0.05). The

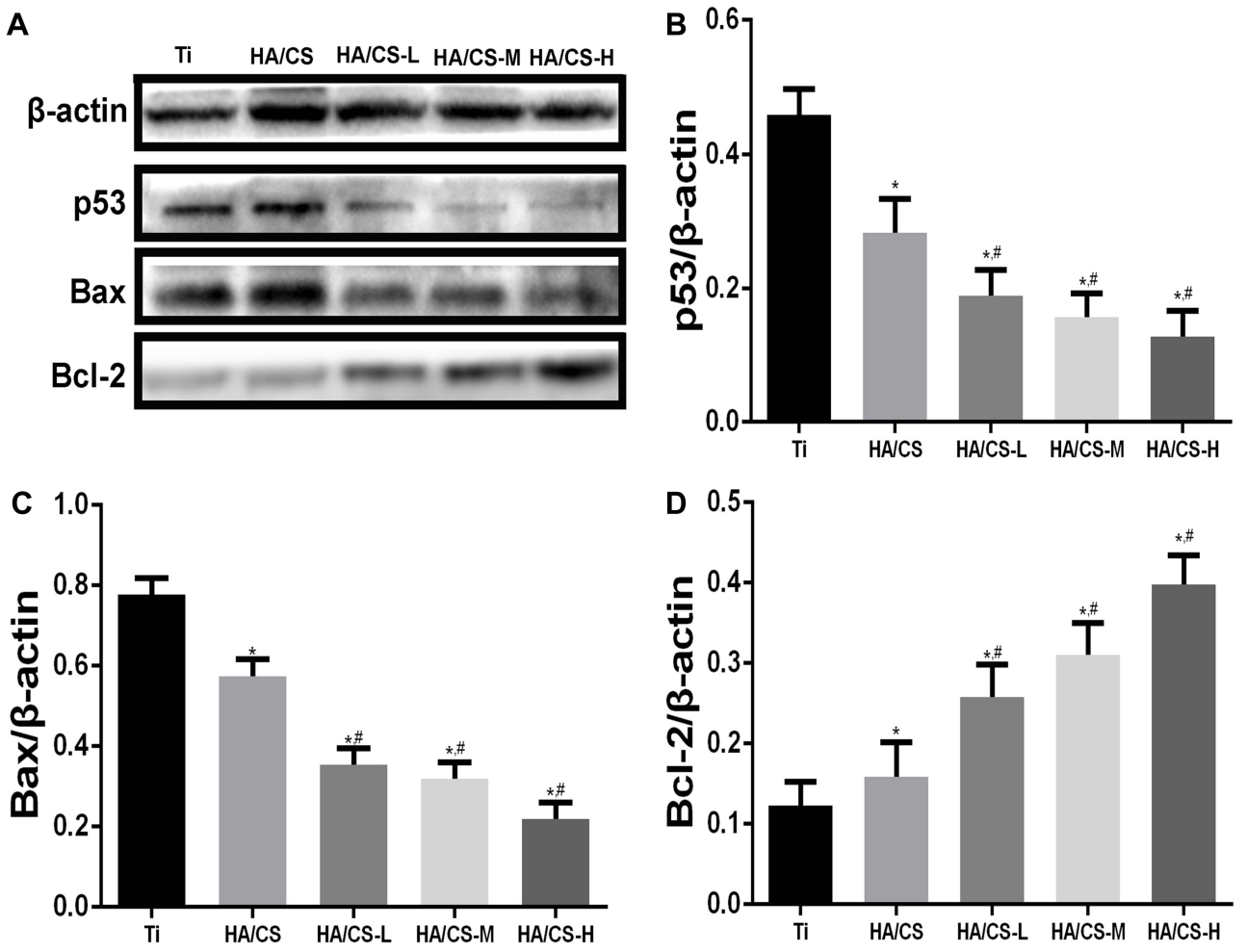

Figure 8 PAC inhibit p53 pathway in the H_2O_2-induced apoptosis.

Notes: (**A**): Western blot analysis of p53, Bax, and Bcl-2 in MC3T3-E1 cells post-treatment of H_2O_2 and PAC; (**B, C & D**): Percentage of p53, Bax, Bcl-2 in MC3T3-E1 cells post-treatment of H_2O_2 and PAC; Data are expressed as mean ± SD (n=3). *A statistical significance compared to the Ti group ($P<0.05$). #A statistical significance compared to the HA/CS multilayer group ($P<0.05$).

Abbreviations: CS, chitosan; HA, hyaluronic acid; HA/CS-H, proanthocyanidins-high dose; HA/CS-L, proanthocyanidins-low dose; HA/CS-M, proanthocyanidins-middle dose.

bone formation around the native bone in the PAC-loaded group was much more evident than that around the implant in the Ti group. These results indicate that the implants coated with PAC had a faster regeneration rate than the blank Ti implant.

Discussion

The cause of aseptic loosening is not well understood but one prominent and well-accepted theory suggests that metal wear-debris particles arising from the articulating surfaces at the implant-bone interfaces lead to an inflammatory response in the bone tissue near and around the prosthesis that culminates in bone loss and loosening of the implant.[32,33] However, recent work has shown that the electrochemical oxidation and reduction processes that occur at metallic implant surfaces (Ti-based biomaterials and implants included) have a profound effect on the local surrounding tissues and the downstream inflammatory response and oxidative stress reactions is the major cause of failure of the implants.[7,8,34] Reactive oxygen species (ROS) including highly reactive superoxide anion ($O^{2\bullet-}$) and hydrogen peroxide (H_2O_2), are normal metabolic byproducts that play important roles in the inflammatory response serving as both signaling and effector molecules,[10] and cause osteoblast apoptosis.[35] Reactive oxygen intermediates produced at implant-bone interfaces serve as strong chemoattractants for the recruitment of immune cells leading to surrounding tissue damage and fibrosis, whilst ROS produced by immune cells can directly lead to the corrosion of the implants further aggravating aseptic loosening.[9,11]

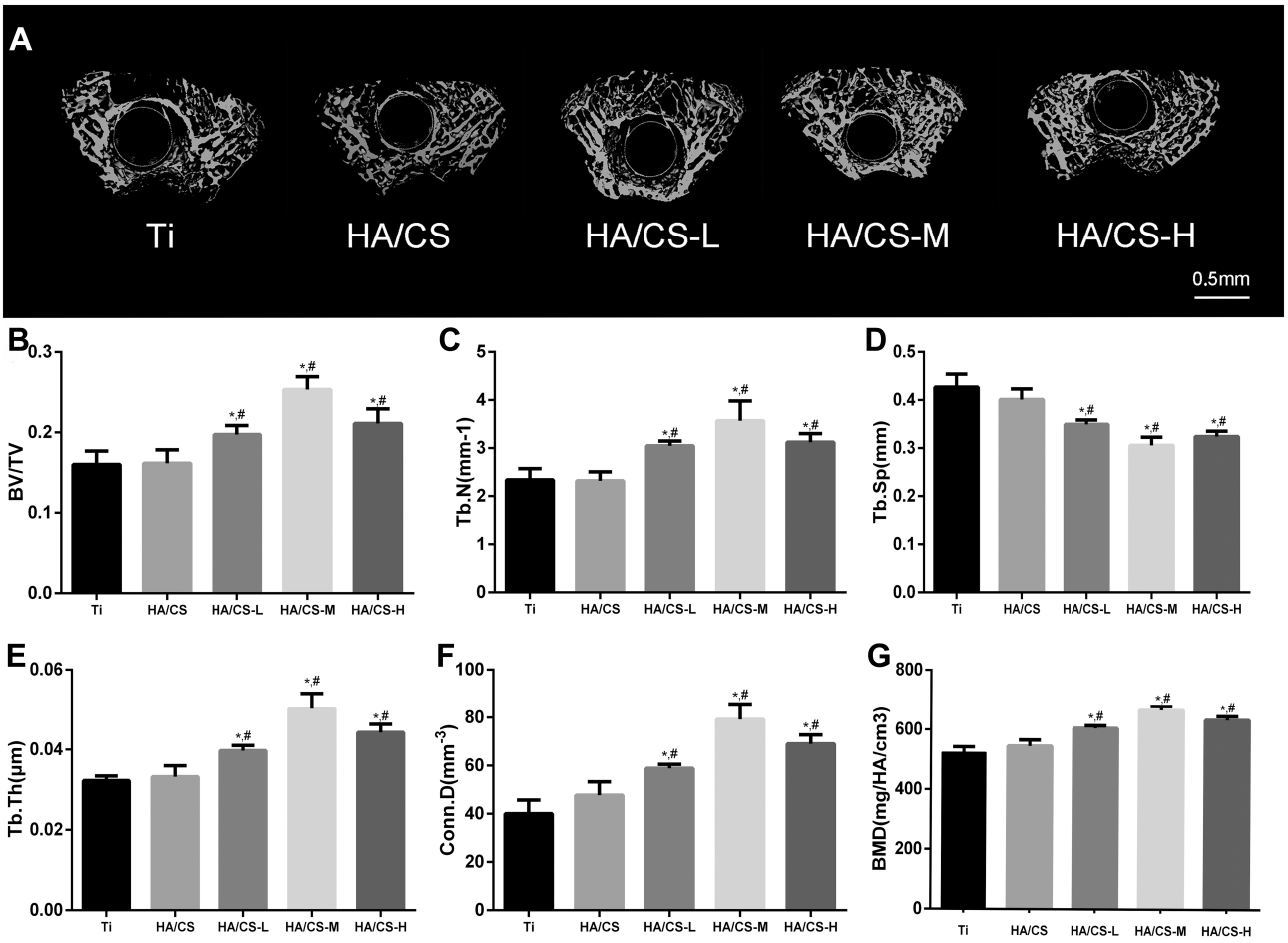

Figure 9 Micro-CT reconstructed and quantitative analysis of distal femur at 2 weeks after implantation.
Notes: (**A**) 3-D image of distal femur bone structure in both Ti rats and different concentration PAC-loaded of Ti rats. (**B**) Quantify analysis of bone volume per total volume (BV/TV), (**C**) trabecular number (Tb.N), (**D**) mean trabecular separation (Tb.Sp), (**E**) trabecular thickness (Tb.Th), (**F**) mean connective density (Conn.D), and (**G**) bone mineral density (BMD) for each group at 2 weeks. Data are expressed as mean ± SD (n=3), *A statistical significance compared to the Ti group ($P<0.05$). #A statistical significance compared to the HA/CS multilayer group ($P<0.05$).
Abbreviations: HA/CS-H, proanthocyanidins-high dose; HA/CS-L, proanthocyanidins-low dose; HA/CS-M, proanthocyanidins-middle dose.

To reduce the deleterious effects of oxidative stress on surrounding tissues and cells, improve osteo-conductivity, osteo-inductivity and overall osteo-integration for the extension of implant lifespan, various coating strategies to supplement the function of current Ti implants have been extensively investigated.[36–38] In this study, we utilized a layer-by-layer (LBL) coating method for the surface modification of pure Ti substrates with several promising biomaterials including polyethylenimine polymers (PEI), hyaluronic acid (HA), chitosan (CS), and proanthocyanidins (PAC), and investigated their osteo-inductivity potential in vitro and in vivo. The LBL electrostatic deposition methodology allows multi-layered coating of biomaterials, by the deposition of different biomaterial on a substrate of subsequent layers.

PEI was chosen as the base layer for coating the Ti substrate surface in preparation of LBL deposition due to its cationic nature, inherent high binding forces, and efficient carrier for drug delivery.[39] Additionally, PEI has shown potent and broad-spectrum antibacterial features an important consideration for warding off implant-related infections and prolonging the effective life of the prosthetic implants. To this layer of PEI, we deposited several bilayers of HA/CS with or without PAC loading. HA is a polyanionic polysaccharide that provides excellent lubricity, anti-bacterial effects, and ability to initiate early- and long-range engagement between cells and substrates. HA also demonstrates high hydration capacity that leads to coatings with high surface energy.[40–42] Chitosan is a polycationic polysaccharide that possesses potent anti-bacterial properties and osteoblast bone formation enhancing effects thus, of particular importance to improve osteo-integration of the coated Ti substrates.[43–45] Furthermore, it has been shown that HA/CS coatings increase surface ionic nature

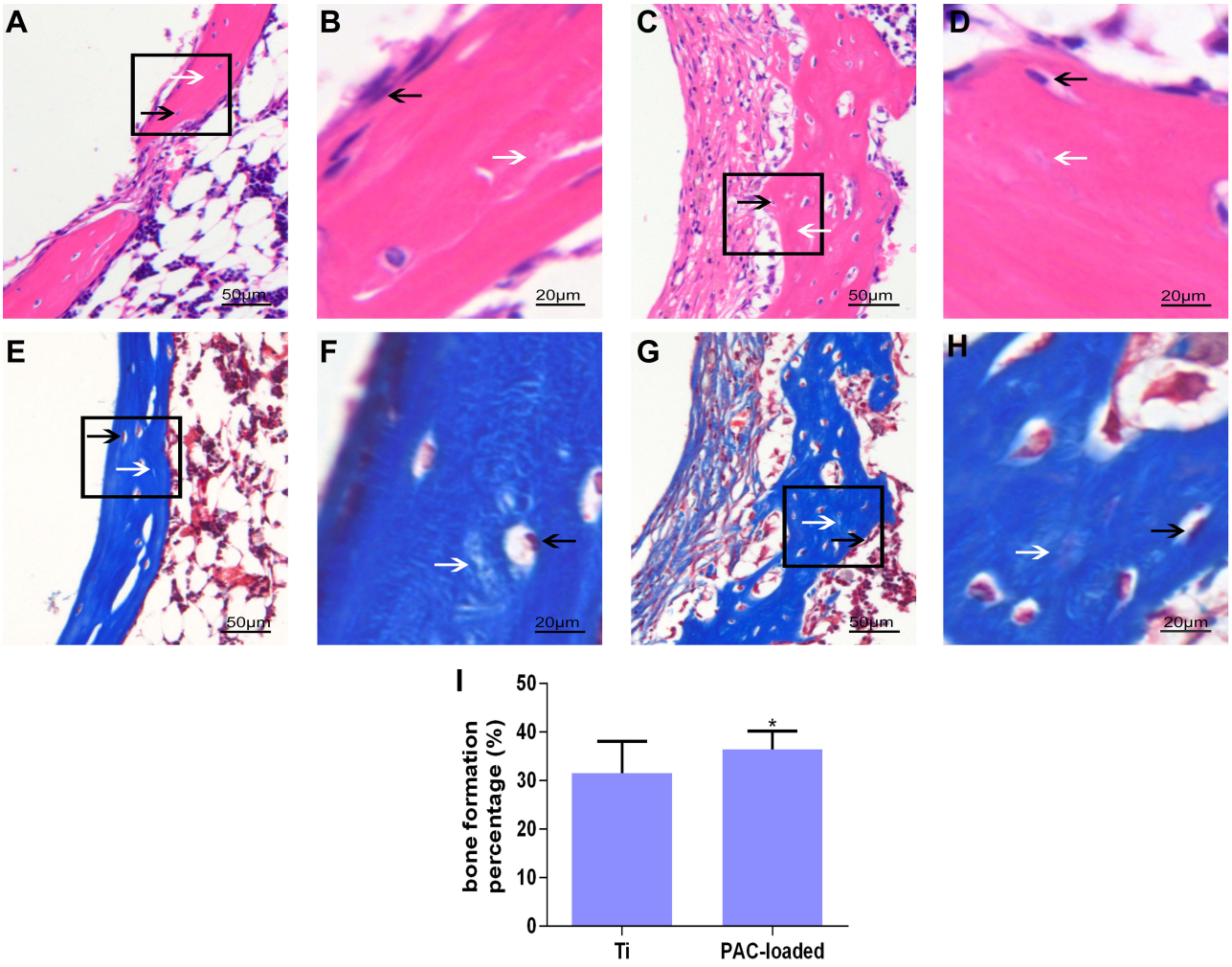

Figure 10 Histological analysis of the decalcification samples around Ti (**A, B, E, F**) and PAC-loaded (**C, D, G, H**) implants.
Notes: (**A-D**) H&E staining; (**E-H**) Masson staining; (**I**) BF %. B, D, F and H depict zoomed areas of black box in A, C, E and G, respectively. Bars indicate 50 μm (**A, C, E, G**) and 20 μm (**B, D, F, H**). The black arrow denotes new bone formation; white arrow denotes osteoblast cell. Histological morphology analyses based on H&E staining after 2 weeks implantation was expressed as was BF % and shown in (**I**). Data are expressed as mean ± SD (n=3), *A statistical significance compared to the Ti group ($P<0.05$).
Abbreviations: PAC, proanthocyanidins; Ti, titanium; BF%, bone formation percent.

and hydrophilicity for enhanced cell adhesion and osteoblast differentiation.[46] PAC are a group of naturally occurring polyphenolic bioflavonoids and possess potent anti-oxidant effects.[14,15] More importantly, owing to its anti-oxidant effects, PAC have shown to be protective against osteoporosis by stimulating osteoblast bone formation and regulating osteoclast bone resorption, as well as alleviating bone destruction in inflammatory autoimmune arthritis.[20] The incorporation of PAC onto the HA/CS layers was achieved via the electrostatic interaction between the reactive negative hydroxyl radical of PAC with the positive amine groups of CS leading to the encapsulation of PAC in the micro-interspaces of 3D HA/CS network.[47]

Consistent with these biological effects, the functionalization of the above biomaterials as a multi-layered coating on Ti substrates providing promising results. Not only were the fabricated Ti substrates well tolerated by MC3T3-E1 pre-osteoblastic cells, loading of PAC onto the HA/CS multi-layer significantly enhanced the proliferation and osteogenic differentiation of MC3T3-E1 pre-osteoblastic cells even under conditions of H_2O_2-induced oxidative stress in vitro. We believe this effect is attributed to two favourable properties of our functionalized Ti substrate. Firstly, the incorporation of both HA and CS (both of which are hydrophilic substrates) onto the Ti substrate significantly increased the hydrophilicity (decreased water contact angle) of the Ti substrate surface. High hydrophilicity of substrates has been shown to be a desirable trait for cell adhesion by increasing the contact area between substrate surface

and the cell, and to promote osteo-conductivity.[31,48,49] Although PAC incorporation reduced hydrophilicity compared to HA/CS substrates alone, the contact surface was still markedly more hydrophilic than uncoated pure Ti substrates. Secondly, the controlled and sustained release of PAC from the HA/CS substrates will have provided the necessary means for the cells to combat the deleterious effects of H_2O_2-induced oxidative stress. HA/CS multi-layer has been shown to exhibit high loading capacity allowing the controlled release of incorporated agents to achieve a long-term effect.[50] The release of PAC from a multi-layered HA/CS system can occur by the diffusion through the layers and/or by the degradation of the weakly attached surface layers. Sustained PAC release was measured for up to 14 days which we believe was sufficient in conveying protection against generated ROS species, improving cellular survival, and osteogenic potential. The Western blotting results suggested that HA/CS-PAC surface could attenuate the ROS-induced down-regulation of anti-apoptotic related protein contents, and overproduction of pro-apoptotic critical executioners.

These favourable in vitro outcomes also translated to promising in vivo results. Previous reports have suggested that the formation of new bone is most active in the early post-operative stage.[51] Thus for our in vivo model, we selected two weeks postoperatively as the time-point for evaluation of the various Ti substrates on bone remodeling. Micro-CT analysis of femoral bone tissues following femoral intramedullary implantation model showed that Ti substrates multi-layered with HA/CS and PAC significantly improved osteo-integration with enhanced bone volume around the implant. Similarly, histological examination provided clear evidence for new bone formation around implant-bone interface with significant reduction in inflammatory response and tissue fibrosis was also noted when compared to uncoated pure Ti substrates. The sustained released of PAC from the multi-layered HA/CS substrate would have no doubt contributed favorably against potential ROS-induced inflammatory response following surgery. The p53 signaling pathway[52,53] and the subsequent downstream induction of the pro-apoptotic protein Bax[54,55] are widely known for its role in H_2O_2-induced apoptosis. In this study, we showed that cells cultured on HA/CS-PAC substrates were protected against the deleterious effects of H_2O_2 at least in part due to the suppression of the p53-Bax-mediated apoptotic program. We believe that such effect is likely attributed to the anti-oxidant, anti–inflammatory and osteogenic properties of the multi-layered HA/CS-PAC coating. Both PAC and chitosan have been suggested to alter multiple signaling pathways involved in osteogenesis and inflammation including BMP2/RUNX2, and Wnt/β-catenin, MAPK, NF-kB, and PI3K/Akt signaling pathways.[56,57] However, more in-depth analysis of these pathways will need to be conducted to delineate the underlying molecular mechanism responsible for the effects seen in our study.

Conclusion

The electrochemical redox processes that occur at metallic implant surfaces can exacerbate local inflammatory response and local tissue destruction leading to failure of the implants. Our study has provided evidence for the effective use of the LBL assembly for the multi-layering of HA/CS-PAC coating onto Ti or Ti-based surfaces for the enhancement of implant osseo-integration, promoting osteogenesis and local bone formation around the implant by mitigating ROS-mediated inflammatory response and p53-Bax-mediated apoptosis, so as to prolong the stability and lifespan of the implant. This study provides new insights for future applications in the field of joint arthroplasty. Future research is needed to further determine the optimal drug concentration on the surface of the implant and to determine the underlying molecular mechanism responsible for the osteogenic and anti–inflammatory effects.

Ethical Approval

Statement of ethical approval animals was handled with the approval of the Animal Experimentation Ethics Committee of Second Affiliated Hospital of Wenzhou Medical University.

Acknowledgments

This work was funded by a research grant to Science and Technology Department of Zhejiang Province (Grant No.:2016C37122), National Natural Science Foundation of China (Grant No.:81772348), National Natural Science Foundation of China (41506091), and Wenzhou Science & Technology Bureau (Y20190021).

Disclosure

The authors report no conflicts of interest in this work.

References

1. Sundfeldt M, Carlsson LV, Johansson CB, Thomsen P, Gretzer C. Aseptic loosening, not only a question of wear: a review of different theories. *Acta Orthop*. 2006;77(2):177–197. doi:10.1080/17453670610045902

2. Das K, Bose S, Bandyopadhyay A. TiO2 nanotubes on Ti: influence of nanoscale morphology on bone cell-materials interaction. *J Biomed Mater Res A*. 2009;90(1):225–237. doi:10.1002/jbm.a.32088
3. Thakur VK, Voicu SI. Recent advances in cellulose and chitosan based membranes for water purification: a concise review. *Carbohydr Polym*. 2016;146:148–165. doi:10.1016/j.carbpol.2016.03.030
4. Salehi E, Daraei P, Arabi Shamsabadi A. A review on chitosan-based adsorptive membranes. *Carbohydr Polym*. 2016;152:419–432. doi:10.1016/j.carbpol.2016.07.033
5. Bearinger JP, Orme CA, Gilbert JL. Effect of hydrogen peroxide on titanium surfaces: in situ imaging and step-polarization impedance spectroscopy of commercially pure titanium and titanium, 6-aluminum, 4-vanadium. *J Biomed Mater Res A*. 2003;67(3):702–712. doi:10.1002/jbm.a.10116
6. Ehrensberger MT, Sivan S, Gilbert JL. Titanium is not "the most biocompatible metal" under cathodic potential: the relationship between voltage and MC3T3 preosteoblast behavior on electrically polarized cpTi surfaces. *J Biomed Mater Res A*. 2010;93(4):1500–1509. doi:10.1002/jbm.a.32622
7. Sivan S, Kaul S, Gilbert JL. The effect of cathodic electrochemical potential of Ti-6Al-4V on cell viability: voltage threshold and time dependence. *J Biomed Mater Res*. 2013;101(8):1489–1497. doi:10.1002/jbm.b.32970
8. Gilbert JL, Sivan S, Liu Y, Kocagöz SB, Arnholt CM, Kurtz SM. Direct in vivo inflammatory cell-induced corrosion of CoCrMo alloy orthopedic implant surfaces. *J Biomed Mater Res A*. 2015;103(1):211–223. doi:10.1002/jbm.a.v103.1
9. Dickinson BC, Chang CJ. Chemistry and biology of reactive oxygen species in signaling or stress responses. *Nat Chem Biol*. 2011;7(8):504–511. doi:10.1038/nchembio.607
10. Tiganis T. Reactive oxygen species and insulin resistance: the good, the bad and the ugly. *Trends Pharmacol Sci*. 2011;32(2):82–89. doi:10.1016/j.tips.2010.11.006
11. Nathan C, Cunningham-Bussel A. Beyond oxidative stress: an immunologist's guide to reactive oxygen species. *Nat Rev Immunol*. 2013;13(5):349–361. doi:10.1038/nri3423
12. Anderson JM. Biological responses to materials. *Annu Rev Mater Res*. 2001;31(1):81–110. doi:10.1146/annurev.matsci.31.1.81
13. Anderson JM, Rodriguez A, Chang DT. Foreign body reaction to biomaterials. *Semin Immunol*. 2008;20(2):86–100. doi:10.1016/j.smim.2007.11.004
14. Nandakumar V, Singh T, Katiyar SK. Multi-targeted prevention and therapy of cancer by proanthocyanidins. *Cancer Lett*. 2008;269(2):378–387. doi:10.1016/j.canlet.2008.03.049
15. Hümmer W, Schreier P. Analysis of proanthocyanidins. *Mol Nutr Food Res*. 2008;52(12):1381–1398. doi:10.1002/mnfr.v52:12
16. Bagchi D, Bagchi M, Stohs S, Ray SD, Sen CK, Preuss HG. Cellular protection with proanthocyanidins derived from grape seeds. *Ann N Y Acad Sci*. 2002;957:260–270. doi:10.1111/nyas.2002.957.issue-1
17. Prasad R, Vaid M, Katiyar SK. Grape proanthocyanidin inhibit pancreatic cancer cell growth in vitro and in vivo through induction of apoptosis and by targeting the PI3K/Akt pathway. *PLoS One*. 2012;7(8):e43064.
18. Tofani I, Maki K, Kojima K, Kimura M. Beneficial effects of grape seed proanthocyanidins extract on formation of tibia bone in low-calcium feeding rats. *Pediatr Dent J*. 2004;14(1):47–53. doi:10.1016/S0917-2394(04)70008-7
19. Park J-S, Park M-K, Oh H-J, et al. Grape-seed proanthocyanidin extract as suppressors of bone destruction in inflammatory autoimmune arthritis. *PLoS One*. 2012;7(12):e51377. doi:10.1371/journal.pone.0051377
20. Tanabe S, Santos J, La VD, Howell AB, Grenier D. A-type cranberry proanthocyanidins inhibit the RANKL-dependent differentiation and function of human osteoclasts. *Molecules*. 2011;16(3):2365–2374. doi:10.3390/molecules16032365
21. Zhang Z, Zheng L, Zhao Z, Shi J, Wang X, Huang J. Grape seed proanthocyanidins inhibit H2O2-induced osteoblastic MC3T3-E1 cell apoptosis via ameliorating H2O2-induced mitochondrial dysfunction. *J Toxicol Sci*. 2014;39(5):803–813. doi:10.2131/jts.39.803
22. Oršolić N, Nemrava J, Jeleč Ž, et al. The beneficial effect of proanthocyanidins and icariin on biochemical markers of bone turnover in rats. *Int J Mol Sci*. 2018;19(9). doi:10.3390/ijms19092746
23. Smith RC, Riollano M, Leung A, Hammond PT. Layer-by-layer platform technology for small-molecule delivery. *Angew Chem Int Ed Engl*. 2009;48(47):8974–8977. doi:10.1002/anie.200902782
24. Jere D, Jiang HL, Arote R, et al. Degradable polyethylenimines as DNA and small interfering RNA carriers. *Expert Opin Drug Deliv*. 2009;6(8):827–834. doi:10.1517/17425240903029183
25. Wright NC, Looker AC, Saag KG, et al. The recent prevalence of osteoporosis and low bone mass in the United States based on bone mineral density at the femoral neck or lumbar spine. *J Bone Mineral Res*. 2014;29(11):2520–2526. doi:10.1002/jbmr.2269
26. Hartmann H, Hossfeld S, Schlosshauer B, et al. Hyaluronic acid/chitosan multilayer coatings on neuronal implants for localized delivery of siRNA nanoplexes. *J Control Release*. 2013;168(3):289–297. doi:10.1016/j.jconrel.2013.03.026
27. Jeon S, Yoo CY, Park SN. Improved stability and skin permeability of sodium hyaluronate-chitosan multilayered liposomes by Layer-by-Layer electrostatic deposition for quercetin delivery. *Colloids Surf B*. 2015;129:7–14. doi:10.1016/j.colsurfb.2015.03.018
28. Song W, Song X, Yang C, et al. Chitosan/siRNA functionalized titanium surface via a layer-by-layer approach for in vitro sustained gene silencing and osteogenic promotion. *Int J Nanomedicine*. 2015;10:2335–2346. doi:10.2147/IJN.S76513
29. Benzie IF, Strain JJ. The ferric reducing ability of plasma (FRAP) as a measure of "antioxidant power": the FRAP assay. *Anal Biochem*. 1996;239(1):70–76. doi:10.1006/abio.1996.0292
30. Gu XN, Xie XH, Li N, Zheng YF, Qin L. In vitro and in vivo studies on a Mg-Sr binary alloy system developed as a new kind of biodegradable metal. *Acta Biomater*. 2012;8(6):2360–2374. doi:10.1016/j.actbio.2012.02.018
31. Zuldesmi M, Waki A, Kuroda K, Okido M. Hydrothermal treatment of titanium alloys for the enhancement of osteoconductivity. *Mater Sci Eng C*. 2015;49:430–435. doi:10.1016/j.msec.2015.01.031
32. Thiele K, Perka C, Matziolis G, Mayr HO, Sostheim M, Hube R. Current failure mechanisms after knee arthroplasty have changed: polyethylene wear is less common in revision surgery. *J Bone Joint Surg*. 2015;97(9):715–720. doi:10.2106/JBJS.M.01534
33. Pivec R, Johnson AJ, Mears SC, Mont MA. Hip arthroplasty. *Lancet*. 2012;380(9855):1768–1777. doi:10.1016/S0140-6736(12)60607-2
34. Haeri M, Wöllert T, Langford GM, Gilbert JL. Voltage-controlled cellular viability of preosteoblasts on polarized cpTi with varying surface oxide thickness. *Bioelectrochemistry*. 2013;94:53–60. doi:10.1016/j.bioelechem.2013.06.002
35. Azizi B, Ziaei A, Fuchsluger T, Schmedt T, Chen Y, Jurkunas UV. p53-regulated increase in oxidative-stress–induced apoptosis in Fuchs endothelial corneal dystrophy: a native tissue model. *Invest Ophthalmol Vis Sci*. 2011;52(13):9291–9297. doi:10.1167/iovs.11-8312
36. Cho Y-D, Kim S-J, Bae H-S, et al. Biomimetic approach to stimulate osteogenesis on titanium implant surfaces using fibronectin derived oligopeptide. *Curr Pharm Des*. 2016;22(30):4729–4735. doi:10.2174/1381612822666160203143053
37. Lee J-Y, Nam S-H, Im S-Y, et al. Enhanced bone formation by controlled growth factor delivery from chitosan-based biomaterials. *J Control Release*. 2002;78(1–3):187–197. doi:10.1016/S0168-3659(01)00498-9
38. Park IS, Lee MH, Bae TS, Seol KW. Effects of anodic oxidation parameters on a modified titanium surface. *J Biomed Mater Res*. 2008;84B(2):422–429. doi:10.1002/(ISSN)1552-4981

39. Cooper SL, Glenn JS, Greenberg HB. Host–microbe interactions: viruses Lessons in defense: hepatitis C, a case study. *Curr Opin Microbiol*. 2001;4(2):222. doi:10.1016/S1369-5274(00)00192-2
40. Pitt WG, Morris RN, Mason ML, Hall MW, Luo Y, Prestwich GD. Attachment of hyaluronan to metallic surfaces. *J Biomed Mater Res A*. 2004;68(1):95–106. doi:10.1002/jbm.a.10170
41. Junter G-A, Thébault P, Lebrun L. Polysaccharide-based antibiofilm surfaces. *Acta Biomater*. 2016;30:13–25. doi:10.1016/j.actbio.2015.11.010
42. Romanò CL, Vecchi E, Bortolin M, Morelli I, Drago L. Hyaluronic acid and its composites as a local antimicrobial/antiadhesive barrier. *J Bone Joint Infect*. 2017;2(1):63–72. doi:10.7150/jbji.17705
43. Arpornmaeklong P, Suwatwirote N, Pripatnanont P, Oungbho K. Growth and differentiation of mouse osteoblasts on chitosan-collagen sponges. *Int J Oral Maxillofac Surg*. 2007;36(4):328–337. doi:10.1016/j.ijom.2006.09.023
44. Hamilton V, Yuan Y, Rigney DA, et al. Bone cell attachment and growth on well-characterized chitosan films. *Polym Int*. 2007;56(5):641–647. doi:10.1002/(ISSN)1097-0126
45. Jing YJ, Hao YJ, Qu H, Shan Y, Li DS, Du RQ. Studies on the antibacterial activities and mechanisms of chitosan obtained from cuticles of housefly larvae. *Acta Biol Hung*. 2007;58(1):75–86. doi:10.1556/ABiol.57.2007.1.7
46. Park JH, Schwartz Z, Olivares-Navarrete R, Boyan BD, Tannenbaum R. Enhancement of surface wettability via the modification of microtextured titanium implant surfaces with polyelectrolytes. *Langmuir*. 2011;27(10):5976–5985. doi:10.1021/la2000415
47. Chen J, Pan P, Zhang Y, Zhong S, Zhang Q. Preparation of chitosan/nano hydroxyapatite organic-inorganic hybrid microspheres for bone repair. *Colloids Surf B*. 2015;134:401–407. doi:10.1016/j.colsurfb.2015.06.072
48. Altankov G, Groth T. Reorganization of substratum-bound fibronectin on hydrophilic and hydrophobic materials is related to biocompatibility. *J Mater Sci*. 1994;5(9–10):732–737.
49. Curtis AS, Forrester JV, McInnes C, Lawrie F. Adhesion of cells to polystyrene surfaces. *J Cell Biol*. 1983;97(5 Pt 1):1500–1506. doi:10.1083/jcb.97.5.1500
50. Macdonald ML, Samuel RE, Shah NJ, Padera RF, Beben YM, Hammond PT. Tissue integration of growth factor-eluting layer-by-layer polyelectrolyte multilayer coated implants. *Biomaterials*. 2011;32(5):1446–1453. doi:10.1016/j.biomaterials.2010.10.052
51. Förster Y, Rentsch C, Schneiders W, et al. Surface modification of implants in long bone. *Biomatter*. 2012;2(3):149–157. doi:10.4161/biom.21563
52. Ryer EJ, Sakakibara K, Wang C, et al. Protein kinase C delta induces apoptosis of vascular smooth muscle cells through induction of the tumor suppressor p53 by both p38-dependent and p38-independent mechanisms. *Journal of Biological Chemistry*. 2005;280(42):35310–35317.
53. Son Y-O, Lee J-C, Hitron JA, Pan J, Zhang Z, Shi X. Cadmium induces intracellular Ca2+-and H2O2-dependent apoptosis through JNK- and p53-mediated pathways in skin epidermal cell line. *Toxicol Sci*. 2010;113(1):127–137. doi:10.1093/toxsci/kfp259
54. Harsdorf R, Li PF, Dietz R. Signaling pathways in reactive oxygen species-induced cardiomyocyte apoptosis. *Circulation*. 1999;99(22):2934–2941. doi:10.1161/01.CIR.99.22.2934
55. Choi Y-J, Jeong Y-J, Lee Y-J, Kwon H-M, Kang Y-H. (-)Epigallocatechin gallate and quercetin enhance survival signaling in response to oxidant-induced human endothelial apoptosis. *J Nutr*. 2005;135(4):707–713. doi:10.1093/jn/135.4.707
56. Puiggròs F, Salvadó M-J, Bladé C, Arola L. Differential modulation of apoptotic processes by proanthocyanidins as a dietary strategy for delaying chronic pathologies. *Crit Rev Food Sci Nutr*. 2014;54(3):277–291. doi:10.1080/10408398.2011.565456
57. Zhu W, Yin Z, Zhang Q, et al. Proanthocyanidins inhibit osteoclast formation and function by inhibiting the NF-κB and JNK signaling pathways during osteoporosis treatment. *Biochem Biophys Res Commun*. 2019;509(1):294–300. doi:10.1016/j.bbrc.2018.12.125